Arab Journal of Basic and Applied Sciences

ISSN: (Print) 2576-5299 (Online) Journal homepage: https://www.tandfonline.com/loi/tabs20

Microwave assisted synthesis, characterization and investigation of antibacterial activity of 3-(5-(substituted-phenyl)-4,5-dihydro-1*H*-pyrazol-3-yl)-2*H*-chromen-2-one derivatives

Olayinka O. Ajani, Maria M. Akande, Natasha October, Tolutope O. Siyanbola, Damilola V. Aderohunmu, Anuoluwa A. Akinsiku & Shade J. Olorunshola

To cite this article: Olayinka O. Ajani, Maria M. Akande, Natasha October, Tolutope O. Siyanbola, Damilola V. Aderohunmu, Anuoluwa A. Akinsiku & Shade J. Olorunshola (2019) Microwave assisted synthesis, characterization and investigation of antibacterial activity of 3-(5-(substituted-phenyl)-4,5-dihydro-1*H*-pyrazol-3-yl)-2*H*-chromen-2-one derivatives, Arab Journal of Basic and Applied Sciences, 26:1, 362-375, DOI: 10.1080/25765299.2019.1632141

To link to this article: https://doi.org/10.1080/25765299.2019.1632141

ARAB JOURNAL OF BASIC AND APPLIED SCIENCES
2019, VOL. 26, NO. 01, 362–375
https://doi.org/10.1080/25765299.2019.1632141

University of Bahrain
Taylor & Francis
Taylor & Francis Group

ORIGINAL ARTICLE

Microwave assisted synthesis, characterization and investigation of antibacterial activity of 3-(5-(substituted-phenyl)-4,5-dihydro-1*H*-pyrazol-3-yl)-2*H*-chromen-2-one derivatives

Olayinka O. Ajani[a], Maria M. Akande[a], Natasha October[b], Tolutope O. Siyanbola[a], Damilola V. Aderohunmu[a], Anuoluwa A. Akinsiku[a] and Shade J. Olorunshola[c]

[a]Department of Chemistry, Covenant University, CST, Ota, Ogun State, Nigeria; [b]Department of Chemistry, University of Pretoria, Hatfield, South Africa; [c]Department of Biological Sciences, Covenant University, CST, Ota, Ogun State, Nigeria

ABSTRACT

A variety of 3-(5-(substituted-phenyl)-4,5-dihydro-1*H*-pyrazol-3-yl)-2*H*-chromen-2-one derivatives **3a–j** were synthesized through microwave assisted thermal annulation of corresponding α,β-unsaturated ketones (chalcones) **2a–j** via hydrazinolysis. Chalcones **2a–j** were prepared from 3-acetyl-coumarin **1** which was previously accessed by Pechmann condensation reaction of salicylaldehyde. The series of pyrazoline-based coumarin motifs **3a–j** synthesized, were structurally confirmed by analytical and spectral data. They were then evaluated for their antimicrobial activities using agar diffusion method. The result showed that microwave assisted method (MAM) for the reaction was remarkably successful and gave the targeted products **3a–j** in higher yields at shorter reaction times compared to conventional synthetic method (CSM). The results showed that these skeletal frameworks exhibited marked potency as antibacterial agents. The most active antibacterial agent was 3-(5-(4-(diethylamino) phenyl)-4,5-dihydro-1*H*-pyrazol-3-yl)-2*H*-chromen-2-one **3j** with MIC and MBC values of 3.92 ± 0.22 μg/mL and 7.82 ± 0.43 μg/mL respectively.

ARTICLE HISTORY
Received 27 December 2017
Accepted 24 May 2019

KEYWORDS
Microwave synthesis; pyrazoline; coumarin motifs; antibacterial; gentamicin

1. Introduction

In the recent times, green chemistry possesses the spirit of sustainable development and is attracting increasing interest in the 21st century (Yue et al., 2011). Microwave-assisted reactions, as green approaches, have been intensely investigated since the earliest publication of Gedye et al. (1986). This methodology can be included within the concept of Green Chemistry because the strong absorption of microwave irradiation by one component of the reaction would lead to shorter reaction times and improved energy efficiency (de la Hoz et al., 2016). It has led to accelerated eco-friendly synthesis of various titled sulfur-containing (Gümüş & Elemes, 2018) and nitrogen-containing heterocycles (Ajani, Aderohunmu, et al., 2018). Heterocycles are known to be one of the largest areas of research in organic chemistry and medicinal research (Ajani, 2014). Many naturally occurring substances, traditionally used in popular medicines around the world, contain the coumarin moiety (Stefanachi et al., 2018). Some of the natural origins of coumarin moieties are plants such as *Dipteryx odorata*, *Calophyllum sp.* and *Hedysarum multijugum*. Due to their broad ranges of biological activities, they have also enjoyed laboratory preparation both in micro-scale and large-scale media. Coumarin and its fused derivatives have been reported to possess diverse pharmacological activities such as antimicrobial (Widelski et al., 2018), anticancer (Bouhenna et al., 2018), anti-inflammatory (Chavan & Hosamani, 2018), anti-HIV (Srivastav et al., 2018), antioxidant (Pérez-Cruz et al., 2018), antimalarial (Hu et al., 2018), antitumor (Amin et al., 2018), anti-HCV (Peng et al., 2013), antihyperlipidemic (Iyer & Patil, 2014) and antitubercular (Patel et al., 2013) activities.

Furthermore, muscle relaxant and sedative hypnotic activities of extract containing 4-hydroxycoumarin has been reported (Muhammad et al., 2013). A critical analysis of various reports on naturally as well as the synthetically derived coumarin templates with anti-inflammatory activity have been carried out (Bansal et al., 2013). In the recent review by Patil et al. (2013), coumarin moieties was highly projected as Monoamine oxidase (MAO) enzyme inhibitor which is a crucial target for the management of depression and Alzheimer disease. Coumarin framework was reported as new protector of amyloid

CONTACT Olayinka O. Ajani ola.ajani@covenantuniversity.edu.ng
Supplemental data for this article can be accessed here.

beta-induced neurotoxicity through the mitochondrial-dependent pathway (Song et al., 2013). In addition, they are widely used as food additives (Wei et al., 2018), chiroptical (Delcourt et al., 2019), perfumes, cosmetics, pharmaceuticals (Pereira et al., 2018), insecticides, optical brightening agents (Chatterjee & Seth, 2013), dispersed fluorescent and laser dyes (Acar et al., 2015). In a similar manner, the use of pyrazole as precursor for the synthesis of bioactive motifs (El Azab et al., 2019) and evaluation of their chemical behaviours have gained more importance in the recent decades for tumor cell growth inhibition (Cui et al., 2019) and agricultural (Venkateswarlu et al., 2018) applications. The chemistry of carbon–nitrogen double bond of hydrazone is fast becoming the backbone of condensation reaction in benzo-fused *N*-heterocycles (Ajani, Iyaye, et al., 2018), especially, in the synthesis of pyrazole-bearing motifs.

In view of the occurrence of microorganisms' resistance, increase in severe opportunistic microbial infections (Aslam et al., 2018) and the emergence of new diseases, there is a continuous need for the fast synthesis of new bioactive heterocyclic compounds as potential therapeutic agents. The combination of two different and independently linked hybrid compounds can display synergy and result in a pharmacological potency greater than the sum of each individual moiety's potency (Pawel·czyk et al., 2018). Hence, we have herein investigated the microwave assisted synthesis of pyrazoline-linked coumarin as a green synthetic approach to access biologically active coumarin scaffolds. It was envisaged that the pyrazole insertion in coumarin will create a synergistic effect to boost the activity of the titled compounds.

2. Materials and methods

2.1. General condition

All the solvents and reagents used were purchased from Sigma-Aldrich Chemicals, USA except anisaldehyde and benzaldehyde which were obtained from J.T. Baker Chemicals, UK and hydrazine hydrate and piperidine which were obtained from BDH England. Chemicals used were of analytical grade and, were used directly without any further purification. Melting points were determined in open capillary tubes on Stuart melting point apparatus and were uncorrected. The ^{1}H-NMR and ^{13}C-NMR spectral analyses were run using deuterated dimethyl sulfoxide (DMSO-d_6) solvent at 400 MHz and 100 MHz respectively, with Tetramethyl silane (TMS) being used as the internal standard. The machine used was NMR Bruker DPX 400 spectrometer and chemical shifts δ were recorded in parts per million (ppm). The IR spectra were run in solid state using the Bruker FT-IR; while UV-visible spectrophotometric analyses of all the samples were run in dichloromethane (CH_2Cl_2), Dimethyl sulphoxide and acetone using UV-Genesys spectrophotometer. The progress of the reaction and the level of purity of the prepared compounds were routinely checked by Thin Layer Chromatography (TLC) on silica gel plates using different solvent system based on the variation of polarity of the product of interest and the developed plates were visualized under UV light where necessary. In a situation where more than one spots were observed, column chromatography was used as the purification technique. The microwave assisted syntheses were carried out using a CEM Discover monomode oven operating at 2450 MHz monitored by a PC computer and temperature maintained at a constant value (140 °C) within the power modulation of 500 W within a ramp time of 1–3 min. After reaction was completed, solvents were evaporated under reduced pressure using IKA® RV 10 Rotary evaporator.

2.2. Synthetic chemistry procedure

2.2.1. Synthesis of 3-acetyl-coumarin or 3-acetyl-2H-chromen-2-one (1)

A mixture of ethyl acetoacetate (11.5 ml, 90.13 mmol) and salicylaldehyde (8.6 ml, 81.89 mmol) was catalyzed with piperidine (0.2 ml, 1.64 mmol), and heated under reflux for a period of 20 min to produce a crude solid mass of 3-acetyl-coumarin (TLC monitored). The crude solid was recrystallized from methanol to afford yellow crystal of pure 3-acetyl-coumarin, **1** (15.48 g, 99.6%). ^{1}H-NMR ($CDCl_3$, 400 MHz) δ: 2.27 (s, 3 H, CH_3), 7.42–7.84 (m, 4 H, Benzofused coumarin-H), 8.57 (s, 1 H, Coumarin-H). ^{13}C-NMR ($CDCl_3$, 100 Hz) δ_C: 198.7 (C = O), 159.4 (C = O), 153.0, 137.4, 131.2, 128.3, 127.9, 125.4, 118.1, 116.1, 29.6 (CH_3) ppm. DEPT 135 NMR: +ve signals 137.4, 131.2, 127.9, 125.4, 116.1, 29.6 (CH_3) ppm. +ve signals nil. MS: m/z 188 (M^+, 80%), 145 (100%), 94 (50%). UV-Visible spectral data $\rightarrow \lambda_{max}$ (Log ε): 216 (5.29), 236 (4.65), 288 (4.57), 327 (4.57), 348 (4.49), 355 (4.24), 369 (4.01). IR (KBr): 2925 (CH aliphatic), 1746 (C = O ester), 1685 (C = O), 1606 (C = C), 1369 (C-O) cm^{-1}.

2.2.2. Microwave assisted synthesis of 3-cinnamoyl-2H-chromen-2-one (2a)

Equimolar amount of 3-acetyl-coumarin (3.00 g, 16.00 mmol) and benzaldehyde (1.62 mL, 16.00 mmol) were mixed together followed by addition of a catalytic amount of piperidine (5 drops). The mixture was swirled and irradiated in microwave oven until the reaction was completed (1 min). The progress of reaction was monitored using Thin Layer Chromatography (TLC) (eluting solvent: Dichloromethane) before the reaction was terminated. The product was recrystallized from ethanol to afford compound **2a.** The same

procedure for synthesis of **2a** was repeated for other benzaldehyde derivatives to afford **2b–j.** The detail of the spectral data of reactive intermediates **2a–j** is as presented in supplementary material.

2.2.3. General procedure for synthesis of 3-(substituted-phenyl-4,5-dihydro-1H-pyrazol-3-yl)-2H-chromen-2-one (3a–j)

Method A (MAM): Hydrazine hydrate (0.36 mL, 7.20 mmol) was added to each of the compounds 3-(3-(substituted-phenyl)acryloyl)-2*H*-chromen-2-one **2a–j** (7.20 mmol) in sealed tube and the mixture was irradiated in microwave oven for a required period of time. Upon reaction completion as indicated by TLC monitoring, the resulting mixture was cooled to ambient temperature to give a crude compound which was recrystallized from ethanol. The product was then cooled, filtered and air-dried to afford corresponding pyrazoline-based coumarin **3a–j** in varying percentage yields.

Method B (CSM): Each of the required intermediates 3-(3-(substituted-phenyl)acryloyl)-2*H*-chromen-2-one **2a–j** (7.20 mmol) was dissolved in 20 mL of ethanol in a 250 mL round bottomed quick-fit flask and stirred at room temperature for 5 min. Hydrazine hydrate (0.36 mL, 7.20 mmol) was cautiously added to the solution and the resulting mixture was then heated under reflux via conventional method for a total of 5 to 6 h before the starting material was totally consumed which was an indication of reaction completion (monitored by TLC). The solvent was concentrated and cooled to afford solid which was recrystallized from ethanol/water or column chromatography where necessary to afford the envisaged products **3a–j**.

2.2.3.1. 3-(5-phenyl-4,5-dihydro-1H-pyrazol-3-yl)-2H-chromen-2-one, (3a).

Reagents: 3-Cinnamoyl-2*H*-chromen-2-one **2a** (2.00 g, 7.20 mmol), hydrazine hydrate (0.36 mL, 7.20 mmol), Conditions: MWI for 1½ min, 140 °C. Purification: recrystallization (ethanol). ^{1}H-NMR (DMSO-d$_6$, 400 MHz) δ_H: 8.64 (s, 1 H, Het-H), 7.96–7.94 (d, J = 7.68 Hz, 1 H, Ar-**H**), 7.76–7.72 (t, J = 7.68 Hz, 1 H, Ar-**H**), 7.44–7.40 (m, 2 H, Ar-H), 7.23 (s, 5 H, Ar-**H**), 6.83–6.81 (d, J = 9.64 Hz, 1 H, **NH**-CH), 3.36–3.31 (m, 1 H, CH), 2.59–2.58 (d, J = 4.56 Hz, 2 H, **CH$_2$**-CH). ^{13}C-NMR (DMSO-d$_6$, 100 MHz) δ_C: 195.0 (C = O), 154.0 (C-O), 147.0, 138.3, 136.7, 134.4, 130.7, 128.9, 124.9, 124.3, 123.0, 120.8, 118.1, 116.0, 114.8, 113.5, 58.4 (CH), 45.6 (CH$_2$) ppm. DEPT 135 NMR: +ve signals 147.0, 138.3, 136.7, 134.4, 130.7, 124.9, 123.0, 120.8, 116.0, 114.8, 58.4 (CH) ppm; −ve signal 45.6 (CH$_2$) ppm. UV-Visible spectral data → λ_{max} (Log ε): 221 (3.33), 239 (3.55), 290 (3.63), 353 (3.44). FT-IR (KBr): 3421 (N-H), 3042 (CH aromatic), 2964 (CH aliphatic), 1755 (C = O of ester), 1605 (C = C), 1593 (C = N), 1373 (C-O of ester), 1226 (C-N), 747 (Ar-H) cm^{-1}.

2.2.3.2. 3-(5-(4-(dimethylamino)phenyl)-4,5-dihydro-1H-pyrazol-3-yl)-2H-chromen-2-one (3 b).

Reagents: 3-(3-(4-Dimethylaminophenyl)acryloyl)-2*H*-chromen-2-one **2 b** (2.30 g, 7.20 mmol), hydrazine hydrate (0.36 mL, 7.20 mmol), Conditions: MWI for 1½ min, 140 °C. Purification: recrystallization (ethanol). ^{1}H-NMR (DMSO-d$_6$, 400 MHz) δ_H: 8.64 (s, 1 H, Het-H), 7.96–7.94 (d, J = 7.70 Hz, 1 H, Ar-**H**), 7.76–7.73 (t, J = 7.68 Hz, 1 H, Ar-**H**), 7.60–7.58 (d, J = 8.00 Hz, 2 H, Ar-**H**), 7.46–7.42 (m, 2 H, Ar-H), 7.24–7.22 (d, J = 8.00 Hz, 2 H, Ar-**H**), 6.94–6.91 (d, J = 9.64 Hz, 1 H, **NH**-CH), 3.41–3.36 (m, 1 H, CH), 2.60–2.59 (d, J = 4.58 Hz, 2 H, **CH$_2$**-CH), 2.35 (s, 6 H, **CH$_3$**-N-**CH$_3$**). ^{13}C-NMR (DMSO-d$_6$, 100 MHz) δ_C: 195.0 (C = O), 154.5 (C-O), 147.0, 145.4, 138.3, 136.4, 134.3, 130.7, 129.2, 125.4, 124.2, 122.5, 120.1, 118.1, 116.0, 113.1, 59.4 (CH), 45.8 (CH$_2$), 29.5 (2 × CH$_3$) ppm. DEPT 135 NMR: +ve signals 147.0, 138.3, 136.4, 134.3, 130.7, 125.4, 122.5, 120.1, 116.0, 59.4 (CH), 29.5 (2 × CH$_3$) ppm. −ve signal 45.8 (CH$_2$) ppm. UV-Visible spectral data → λ_{max} (Log ε): 227 (3.06), 257 (3.36), 320 (3.18), 392 (3.57). FT-IR (KBr): 3412 (N-H), 2910 (CH aliphatic), 1746 (C = O of ester), 1601 (C = C), 1584 (C = N), 1364 (C-O of ester), 1228 (C-N), 786 (Ar-H) cm^{-1}.

2.2.3.3. 3-(5-(4-hydroxy-3-methoxyphenyl)-4,5-dihydro-1H-pyrazol-3-yl)-2H-chrom en-2-one (3c).

Reagents: 3-(3-(4-hydroxy-3-methoxyphenyl)acryloyl)-2*H*-chromen-2-one **2c** (2.32 g, 7.20 mmol), hydrazine hydrate (0.36 mL, 7.20 mmol), Conditions: MWI for 2 min, 140 °C. Purification: recrystallization (ethanol). ^{1}H-NMR (DMSO-d$_6$, 400 MHz) δ_H: 8.64 (s, 1 H, Het-H), 8.42 (s, 1 H, Ar-**OH**), 7.96–7.93 (d, J = 8.50 Hz, 1 H, Ar-**H**), 7.76–7.73 (t, J = 7.98 Hz, 1 H, Ar-**H**), 7.57–7.55 (d, J = 7.70 Hz, 1 H, Ar-**H**), 7.44–7.41 (m, 2 H, Ar-H), 7.31–7.29 (d, J = 8.00 Hz, 1 H, Ar-**H**), 7.11–7.09 (d, J = 8.00 Hz, 1 H, Ar-**H**), 6.85–6.83 (d, J = 9.04 Hz, 1 H, **NH**-CH), 3.36–3.31 (m, 1 H, CH), 2.60–2.58 (d, J = 4.98 Hz, 2 H, **CH$_2$**-CH), 2.20 (s, 3 H, O**CH$_3$**). ^{13}C-NMR (DMSO-d$_6$, 100 MHz) δ_C: 195.0 (C = O), 154.5, 147.0, 143.2, 141.0, 138.3, 136.4, 134.3, 130.7, 219.2, 124.9, 124.3, 122.9, 118.1, 116.0, 113.1, 59.4 (CH), 45.8 (CH$_2$), 29.5 (CH$_3$) ppm. DEPT 135 NMR: +ve signals 147.0, 138.3, 136.4, 134.3, 124.9, 122.9, 116.0, 59.4 (CHs), 29.5 (CH$_3$) ppm; −ve signal 45.8 (CH$_2$) ppm. UV-Visible spectral data → λ_{max} (Log ε): 226 (3.20 s), 253 (3.90 s), 282 (3.75 s), 353 (4.016). FT-IR (KBr): 3350 (OH), 2980 (CH aliphatic), 1750 (C = O of ester), 1618 (C = C aromatic), 1572 (C = N), 1374 (C-O of ester), 1225 (C-N), 1044 (C-O of phenol), 747 (Ar-H) cm^{-1}.

2.2.3.4. 3-(5-(4-ethoxyphenyl)-4,5-dihydro-1H-pyrazol-3-yl)-2H-chromen-2-one (3d).

Reagents: 3-(3-(4-Ethoxyphenyl)acryloyl)-2*H*-chromen-2-one **2d** (2.31 g,

7.20 mmol), hydrazine hydrate (0.36 mL, 7.20 mmol), Conditions: MWI for 3 min, 140 °C. Purification: recrystallization (ethanol). ^{1}H-NMR (DMSO-d_6, 400 MHz) δ_H: 8.64 (s, 1 H, Het-H), 7.96–7.93 (d, J = 8.66 Hz, 1 H, Ar-**H**), 7.77–7.74 (t, J = 7.94 Hz, 1 H, Ar-**H**), 7.62–7.60 (d, J = 8.00 Hz, 2 H, Ar-**H**), 7.46–7.40 (m, 2 H, Ar-H), 7.23–7.21 (d, J = 8.00 Hz, 2 H, Ar-**H**), 6.94–6.91 (d, J = 9.14 Hz, 1 H, **NH**-CH), 3.40–3.36 (m, 1 H, CH), 3.12–3.08 (q, J = 8.80 Hz, 2 H, **CH$_2$**-CH$_3$), 2.60–2.55 (d, J = 5.06 Hz, 2 H, **CH$_2$**-CH), 2.35–2.30 (t, J = 8.80 Hz, 2 H, **CH$_3$**-CH$_2$). ^{13}C-NMR (DMSO-d_6, 100 MHz) δ_c: 195.5 (C = O), 154.5, 147.0, 144.7, 140.4, 138.3, 136.7, 134.5, 130.7, 128.8, 124.9, 124.4, 123.0, 120.1, 118.1, 116.0, 59.2 (CH), 52.4 (O-CH$_2$), 45.6 (CH$_2$), 26.4 (CH$_3$) ppm. DEPT 135 NMR: +ve signals 147.0, 138.3, 136.7, 134.5, 124.9, 123.0, 120.1, 116.0, 59.2 (CHs), 26.4 (CH$_3$) ppm; −ve signal 45.6 (CH$_2$) ppm. UV-Visible spectral data → λ_{max} (Log ε): 215 (3.23), 258 (3.75 s), 284 (3.95), 340 (4.05). FT-IR (KBr): 3418 (N-H), 2936 (CH aliphatic), 1747 (C = O of ester), 1610 (C = C aromatic), 1591 (C = N), 1373 (C-O of ester), 1227 (C-N), 746 (Ar-H) cm^{-1}.

2.2.3.5. 3-(5-(4-chlorophenyl)-4,5-dihydro-1H-pyrazol-3-yl)-2H-chromen-2-one (3e). Reagents: 3-(3-(4-Chlorophenyl)acryloyl)-2*H*-chromen-2-one **2e** (2.24 g, 7.20 mmol), hydrazine hydrate (0.36 mL, 7.20 mmol), Conditions: MWI for 1½ min, 140 °C. Purification: recrystallization (ethanol). ^{1}H-NMR (DMSO-d_6, 400 MHz) δ_H: 8.61 (s, 1 H, Het-H), 7.96–7.94 (d, J = 8.00 Hz, 1 H, Ar-**H**), 7.75–7.72 (t, J = 7.98 Hz, 1 H, Ar-**H**), 7.62–7.60 (d, J = 8.20 Hz, 2 H, Ar-**H**), 7.46–7.42 (m, 2 H, Ar-H), 7.26–7.24 (d, J = 8.22 Hz, 2 H, Ar-**H**), 6.94–6.93 (d, J = 7.68 Hz, 1 H, **NH**-CH), 3.41–3.36 (m, 1 H, CH), 2.60–2.57 (d, J = 4.96 Hz, 2 H, **CH$_2$**-CH). ^{13}C-NMR (DMSO-d_6, 100 MHz) δ_c: 194.8 (C = O), 154.3, 151.4, 146.8, 144.6, 140.4, 138.4 (2 × CH), 134.4, 130.3, 128.9, 125.1, 124.3, 123.1 (2 × CH), 118.1, 115.5, 60.2 (CHs), 47.5 (CH$_2$) ppm. DEPT 135 NMR: +ve signals 146.8, 138.4 (2 × CH), 134.4, 130.3, 125.1, 123.1 (2 × CH), 115.5, 60.2 (CHs), ppm; -ve signal 47.5 (CH$_2$) ppm. UV-Visible spectral data → λ_{max} (Log ε): 221 (3.13), 240 (3.30), 256 (3.60 s), 293 (3.84), 358 (3.51). FT-IR (KBr): 3420 (N-H), 2930 (CH aliphatic), 1747 (C = O of ester), 1606 (C = C), 1575 (C = N), 1748 (C = O of ester), 1363 (C-O of ester), 1224 (C-N), 749 (Ar-H) cm^{-1}.

2.2.3.6. 3-(5-(3-hydroxyphenyl)-4,5-dihydro-1H-pyrazol-3-yl)-2H-chromen-2-one (3f). Reagents: 3-(3-(3-Hydroxyphenyl)acryloyl)-2*H*-chromen-2-one **2f** (2.10 g, 7.20 mmol), hydrazine hydrate (0.36 mL, 7.20 mmol), Conditions: MWI for 3 min, 140 °C. Purification: recrystallization (ethanol). ^{1}H-NMR (DMSO-d_6, 400 MHz) δ_H: 8.88 (s, 1 H, Ar-**OH**), 8.61 (s, 1 H, Het-H), 7.96–7.94 (d, J = 8.00 Hz, 1 H, Ar-**H**), 7.76–7.72 (m, 1 H, Ar-**H**), 7.56 (s, 1 H, Ar-**H**), 7.46–7.44 (m, 2 H, Ar-H), 7.31–7.29 (d, J = 8.16 Hz, 1 H, Ar-**H**), 7.11–7.09 (d, J = 8.22 Hz, 1 H, Ar-**H**), 6.85–6.83 (d, J = 7.96 Hz, 1 H, **NH**-CH), 3.36–3.31 (m, 1 H, CH), 2.59–2.57 (d, J = 5.18 Hz, 2 H, **CH$_2$**-CH). ^{13}C-NMR (DMSO-d_6, 100 MHz) δ_c: 195.0, 156.1, 154.5, 152.2, 147.0, 145.1, 141.7, 137.6, 134.4, 130.7, 124.9, 124.3, 121.4, 118.1, 116.0, 113.5, 58.4 (CHs), 46.2 (CH$_2$) ppm. DEPT 135 NMR: +ve signals 152.2, 147.0, 141.7, 137.6, 134.4, 130.7, 124.9, 121.4, 116.0, 58.4 (CHs) ppm; -ve signal 46.2 (CH$_2$) ppm. UV-Visible spectral data → λ_{max} (Log ε): 212 (3.14), 257 (3.47 s), 287 (3.70), 340 (3.62). FT-IR (KBr): 3345 (O-H), 2973 (CH aliphatic), 1750 (C = O of ester), 1615 (C = C), 1579 (C = N), 1371 (C-O of ester), 1220 (C-N), 1043 (C-O of phenol), 750 (Ar-H) cm^{-1}.

2.2.3.7. 3-(5-(4-hydroxyphenyl)-4,5-dihydro-1H-pyrazol-3-yl)-2H-chromen-2-one (3 g). Reagents: 3-(3-(4-Hydroxyphenyl)acryloyl)-2*H*-chromen-2-one **2 g** (2.10 g, 7.20 mmol), hydrazine hydrate (0.36 mL, 7.20 mmol), Conditions: MWI for 1 min, 140 °C. Purification: recrystallization (ethanol). ^{1}H-NMR (DMSO-d_6, 400 MHz) δ_H: 8.80 (s, 1 H, Ar-**OH**), 8.64 (s, 1 H, Het-H), 7.96–7.94 (d, J = 8.00 Hz, 1 H, Ar-**H**), 7.77–7.73 (m, 1 H, Ar-**H**), 7.63–7.60 (d, J = 8.58 Hz, 2 H, Ar-**H**), 7.46–7.42 (m, 2 H, Ar-**H**), 7.25–7.22 (d, J = 8.42 Hz, 2 H, Ar-**H**), 6.84–6.82 (d, J = 7.96 Hz, 1 H, **NH**-CH), 3.41–3.36 (m, 1 H, CH), 2.59–2.57 (d, J = 5.18 Hz, 2 H, **CH$_2$**-CH). ^{13}C-NMR (DMSO-d_6, 100 MHz) δ_c: 195.4, 157.0, 154.9, 151.2, 147.0, 140.4 (2× CH), 142.9, 137.7, 130.7, 127.8, 121.7 (2 × CH), 118.1, 116.0, 113.5, 59.3 (CHs) ppm. DEPT 135 NMR: +ve signals 151.2, 147.0, 140.4 (2× CH), 137.7, 130.7, 121.7 (2 × CH), 116.0, 59.3 (CHs) ppm; -ve signal 47.2 (CH$_2$) ppm. UV-Visible spectral data → λ_{max} (Log ε): 255 (3.83 s), 280 (4.07), 315 (3.93). FT-IR (KBr): 3350 (OH), 2923 (CH aliphatic), 1745 (C = O of ester), 1605 (C = C aromatic), 1588 (C = N), 1372 (C-O of ester), 1226 (C-N), 1044 (C-O of phenol), 747 (Ar-H) cm^{-1}.

2.2.3.8. 3-(5-(3-methoxyphenyl)-4,5-dihydro-1H-pyrazol-3-yl)-2H-chromen-2-one (3 h). Reagents: 3-(3-(3-Methoxyphenyl)acryloyl)-2*H*-chromen-2-one **2 h** (2.21 g, 7.20 mmol), hydrazine hydrate (0.36 mL, 7.20 mmol), Conditions: MWI for 2½ min, 140 °C. Purification: recrystallization (ethanol). ^{1}H-NMR (DMSO-d_6, 400 MHz) δ_H: 8.64 (s, 1 H, Het-H), 7.95–7.93 (d, J = 8.00 Hz, 1 H, Ar-**H**), 7.75–7.72 (m, 1 H, Ar-**H**), 7.56 (s, 1 H, Ar-**H**), 7.46–7.43 (m, 2 H, Ar-**H**), 7.96–7.94 (d, J = 8.00 Hz, 1 H, Ar-**H**), 7.31–7.29 (d, J = 8.42 Hz, 1 H, Ar-**H**), 7.15–7.13 (d, J = 7.88 Hz, 1 H, Ar-**H**), 6.84–6.82 (d, J = 7.96 Hz, 1 H, **NH**-CH), 3.36–3.31 (m, 1 H, CH), 2.60–2.57 (d, J = 5.18 Hz, 2 H, **CH$_2$**-CH), 2.25 (s, 3 H, Ar-OC**H$_3$**). ^{13}C-NMR (DMSO-d_6, 100 MHz) δ_c: 195.0 (C = O), 154.3, 150.9, 146.8, 143.3,

140.8, 138.1, 136.4, 134.4, 127.3, 124.9, 123.1, 118.1, 116.0, 113.8, 111.7, 58.6 (CHs), 46.3 (CH_2), 29.5 (CH_3) ppm. DEPT 135 NMR: +ve signals 150.9, 146.8, 138.1, 136.4, 134.4, 127.3, 124.9, 123.1, 116.0, 111.7, 58.6 (CHs), 29.5 (CH_3) ppm; -ve signal 46.3 (CH_2) ppm. UV-Visible spectral data → λ_{max} (Log ε): 227 (3.05), 258 (2.80 s), 281 (3.62), 353 (3.38). FT-IR (KBr): 3412 (N-H), 2933 (CH aliphatic), 1745 (C = O of ester), 1606 (C = C aromatic), 1576 (C = N), 1365 (C-O of ester), 1224 (C-N), 750 (Ar-H) cm^{-1}.

2.2.3.9. 3-(5-(4-methoxyphenyl)-4,5-dihydro-1H-pyrazol-3-yl)-2H-chromen-2-one (3i). Reagents: 3-(3-(4-Methoxyphenyl)acryloyl)-2*H*-chromen-2-one **2i** (2.21 g, 7.20 mmol), hydrazine hydrate (0.36 mL, 7.20 mmol), Conditions: MWI for 1½ min, 140 °C. Purification: recrystallization (ethanol). ^{1}H-NMR (DMSO-d_6, 400 MHz) δ_H: 8.64 (s, 1 H, Het-H), 7.95–7.93 (d, *J* = 8.48 Hz, 1 H, Ar-**H**), 7.77–7.74 (m, 1 H, Ar-**H**), 7.60–7.58 (d, *J* = 8.00 Hz, 2 H, Ar-**H**), 7.46–7.40 (m, 2 H, Ar-**H**), 7.25–7.23 (d, *J* = 8.00 Hz, 2 H, Ar-**H**), 6.84–6.82 (d, *J* = 8.56 Hz, 1 H, **NH**-CH), 3.36–3.31 (m, 1 H, CH), 2.60–2.59 (d, *J* = 6.18 Hz, 2 H, **CH_2**-CH), 2.20 (s, 3 H, Ar-O**CH_3**). ^{13}C-NMR (DMSO-d_6, 100 MHz) δ_c: 194.5 (C = O), 154.7, 151.6, 147.1, 143.7, 141.0, 138.6, 136.4, 134.4, 127.3, 124.9, 122.7, 118.2, 116.2, 113.5, 111.1, 58.6 (CHs), 46.3 (CH_2), 29.9 (CH_3) ppm. DEPT 135 NMR: +ve signals 147.1, 138.6, 136.4, 134.4, 127.3, 124.9, 122.7, 116.2, 111.1, 58.6 (CHs), 29.9 (CH_3) ppm; -ve signal 46.3 (CH_2) ppm. UV-Visible spectral data → λ_{max} (Log ε): 218 (3.11), 257 (3.36), 320 (3.18), 392 (3.57). FT-IR (KBr): 3443 (N-H of 2°amine), 2930 (CH aliphatic), 1745 (C = O of ester), 1620 (C = C), 1573 (C = N), 1372 (C-O of ester), 1224 (C-N), 761 (Ar-H) cm^{-1}.

2.2.3.10. 3-(5-(4-(diethylamino)phenyl)-4,5-dihydro-1H-pyrazol-3-yl)-2H-chromen-2-one (3j). Reagents: 3-(3-(4-(Diethylamino)phenyl)acryloyl)-2*H*-chromen-2-one **2j** (2.50 g, 7.20 mmol), hydrazine hydrate (0.36 mL, 7.20 mmol), Conditions: MWI for 2½ min, 140 °C. Purification: recrystallization (ethanol). ^{1}H-NMR (DMSO-d_6, 400 MHz) δ_H: 8.69 (s, 1 H, Het-H), 7.95–7.93 (d, *J* = 8.58 Hz, 1 H, Ar-**H**), 7.75–7.73 (m, 1 H, Ar-**H**), 7.58–7.56 (d, *J* = 8.00 Hz, 2 H, Ar-**H**), 7.46–7.42 (m, 2 H, Ar-**H**), 7.22–7.20 (d, *J* = 8.00 Hz, 2 H, Ar-**H**), 6.94–6.91 (d, *J* = 8.56 Hz, 1 H, **NH**-CH), 3.40–3.36 (m, 1 H, CH), 3.14–3.13 (q, *J* = 2.44 Hz, 4 H, 2 × **CH_2**-CH_3), 2.59–2.57 (d, *J* = 6.20 Hz, 2 H, **CH_2**-CH), 2.33–2.32 (t, *J* = 2.44 Hz, 4 H, 2 × **CH_3**-CH_2). ^{13}C-NMR (DMSO-d_6, 100 MHz) δ_c: 195.4 (C = O), 158.0, 154.9, 152.0, 147.0, 142.9, 140.6, 138.2 (2 × CH), 131.0, 128.0, 122.2 (2 × CH), 118.5, 116.4, 109.9, 59.2 (CHs), 50.8 (2 × CH_2), 47.2 (CH_2), 19.5 (2 × CH_3) ppm. DEPT 135 NMR: +ve signals 152.0, 147.0, 138.2 (2 × CH), 131.0, 122.2 (2 × CH), 116.4, 109.9, 59.2 (CHs), 19.5 (2 × CH_3) ppm; -ve signal 50.8 (2 × CH_2), 47.2 (CH_2) ppm. UV-Visible spectral data → λ_{max} (Log ε): 227 (2.92), 226 (3.00), 265 (3.00 s), 398 (3.37), 575 (1.60). FT-IR (KBr): 3420 (N-H), 2969 (CH aliphatic), 1750 (C = O of ester), 1601 (C = C aromatic), 1575 (C = N), 1362 (C-O of ester), 1227 (C-N), 747 (Ar-H), 603 (N-H wagging) cm^{-1}.

2.2.4. Antibacterial activity assay

The typed bacterial isolates used obtained from Nigeria Institute of Medical Research include *Staphylococcus aureus* (ATCC 25923), *Klebsiella pneumoniae* (ATCC 13182), *Pseudomonas aeruginosa* (ATCC 15442), and *Escherichia coli* (ATCC 25922) while *Streptococcus faecalis* and *Proteus vulgaris* were locally isolated organisms (LIO) using Analytical Profile Index (API) Kit. All the isolates were further subjected to biochemical tests for confirmation.

2.2.4.1. Antibacterial sensitivity testing of compounds 3a–j. All the synthesized pyrazoline-based coumarins **3a–j** and gentamicin clinical standard were screened for antibacterial activity on six bacterial strains using agar well diffusion method (Ajani et al., 2010). The general sensitivity testing was carried out with medium employed was diagnostic medium agar from Biotech Limited. Addition of about 0.2 mL of the broth culture to 18 mL sterile molten diagnostic sensitivity test agar (Biotech Ltd) was cautiously done and the mixture was cooled down to 45 °C. This mixture was poured into petri dishes which were previously sterilized prior to use and then labeled with respect to the test organisms. The medium was then allowed to set. Sterile cork borer was utilized to bore the necessary numbers of holes into the medium. The wells were made of to the edge of the plate. The wells which were made of about 5 mm to plate edge, were filled up aseptically with the compound dissolved in DMSO. Gentamicin was used as the standard antibacterial agent at a concentration of 1000 µg/mL. Effective diffusion of the antibacterial agents into the medium was achieved by allowing the plate to stand for 1 h, followed by upright incubation at 37 °C for 24 h. Care was taken not to stockpile the plates. Clear zones of inhibition in millimeters indicated the relative susceptibility of the bacteria to the compounds **3a–j** and gentamicin (std.).

2.2.4.2 Determination of minimum inhibitory/bactericidal concentration (MIC and MBC). Serial dilution technique was adopted for the MIC testing (Ajani & Nwinyi, 2010), which was determined on the six bacterial strains namely: *Staphylococcus aureus* (ATCC 25923), *Klebsiella pneumoniae* (ATCC 13182), *Pseudomonas aeruginosa* (ATCC 15442), and *Escherichia coli* (ATCC 25922) while *Streptococcus*

faecalis (LIO) and *Proteus vulgaris* (LIO). Serial dilution was used to achieve the different concentrations (from 500.00 μg/mL to 3.92 μg/mL) of the synthesized compounds via twofold dilution which was prepared in a sterile plate using sterile pipette and then mixed with 18 mL of molten nutrient agar and allowed to set. Having allowed surface of the nutrient agar plate was dried, streaking with overnight broth cultures of the bacteria was performed. The plates were then labeled accordingly and incubated at 37 °C for up to 72 h. Afterward, the incubated plates were consequently assessed for either presence or absence of growth. The smallest concentration of the compounds which prevented the bacterial growth was recorded and regarded as the MIC of the compounds. This detailed technique was similarly repeated replacing the synthesized compound with gentamicin (clinical standard).

MBC Determination: To obtain minimum bactericidal concentration (MBC), 0.1 mL volume was taken from each tube and spread on agar plates. The number of c.f.u was counted after 18–24 h of incubation at 35 °C.

3. Results and discussion

3.1 Chemistry

3.1.1. Synthetic chemistry

Molecular characterization and structural activity relationship (SAR) studies have shown coumarin derivatives to be highly relevant scaffolds in drug design and medicinal research. In the review by Kale and Patwardhan (2014), emphasis was laid on search of coumarins linked with different heterocycles with respect to their diverse array of biological activities. Hence, the pyrazoline moiety was herein used as a linker between the coumarin template and diverse substituted benzene ring in order to evaluate the structure activity relationship study (SAR) for possible future drug development. Thus, in the continuation of our research effort on the synthesis and the medicinal evaluation of coumarin-based heterocycles (Ajani et al., 2016; Ajani & Nwinyi, 2010), we have herein reported the synthesis and antibacterial activity of novel pyrazoline-coumarin **3a-j.** First and foremost, 3-acetyl-coumarin, **1**, which is the essential precursor herein was synthesized by the condensation reaction of salicylaldehyde and ethyl acetoacetate in the presence of catalytic amount of piperidine as shown in Scheme 1. The method of synthesis of 3-acetyl-coumarin was acquired from the standard procedure reported by Ajani & Nwinyi (2010) but was modified by using a solvent-free medium, a high temperature and a very short reaction time which gave a higher yield of 99.5% as compared with yield of 92.6% obtained in the earlier report (Ajani & Nwinyi, 2010). The condensation reaction of 3-acetyl-coumarin with benzaldehyde and its derivatives in the presence of piperidine via microwave irradiation technique resulted in the formation of α,β-unsaturated carbonyl 3-(3-(substituted-phenyl) acryloyl)-2*H*-chromen-2-one **2a–j** (chalcone intermediates) as shown in Scheme 2. These chalcone intermediates **2a–j** were subsequently reacted with hydrazine hydrate in solvent-free medium to give [3 + 2]-cycloaddition products, 4,5-dihydropyrazolo-inserted coumarin, **3a–j** (Scheme 3) which are also herein referred to as pyrazoline-linked coumarins.

Furthermore, comparative study of microwave-assisted synthesis (MAM – Method A) of titled products **3a–j** with that of conventional synthetic method by heating under reflux (CSM – Method B) was carried out and the result is as shown in Figure 1. Since % yield and kinetic are crucial parameters for measuring the efficiency of a synthetic method, then comparative study of microwave-assisted method (MAM) with conventional synthetic method (CSM) was herein evaluated with special attention on those parameters and the result is as shown in Figure 1. The result of the study showed that compound **3a** was obtained in 91% in MAM but was obtained in 88% in CSM; compound **3b** was produced in 77% using MAM whereas the yield reduced to 71% when CSM was used. Similarly, it was observed that MAM consistently gave the rest of the products **3c-j** in higher yields than the CSM. This was an indication that the MAM was a more efficient method in terms of yield assessment as descriptive indicator of efficiency. All the pyrazoline-based coumarin motifs **3a–j** were obtained at shorter reaction times in MAM (1–3 mins) as compared to CSM (300–360 mins). Thermodynamic justification for faster reaction rate under microwave could be explained by the previous work of Gude et al. (2013) who established, by Arrhenius equation, that the reaction rate under microwave was 1000 folds higher than that from conventional heating approach. The result of the physico-chemical parameters of all the synthesized compounds is as shown in Table 1. The molecular weight of all compounds ranged from 188.18 for compound **1** to 361.44 for compound **3j.** From the MAM, the percentage yields of the compounds ranged from 63.93% being the lowest noted in compound **3d** to 99.50% being the highest reported for precursor **1**. It was noticed that slight modification of the earlier reported method for precursor **1** synthesized resulted in the excellent and highest yield in this present study. All the final products were obtained in good to excellent yields within shortest reaction time (1–3 min) under microwave irradiation. This showed that microwave-assisted synthetic route is not only environmentally friendly

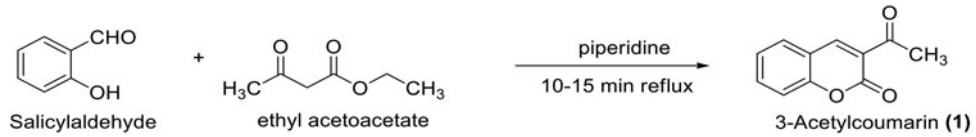

Scheme 1. Equation of reaction for the formation of 3-acetyl-coumarin, **1**

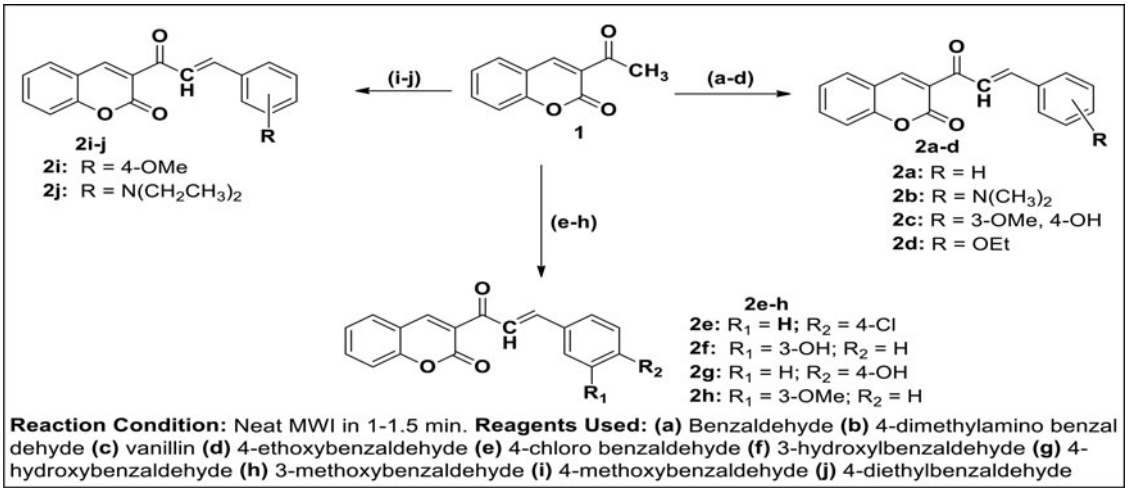

Scheme 2. Microwave-assisted synthesis of chalcones **2a-j** in solvent-free medium

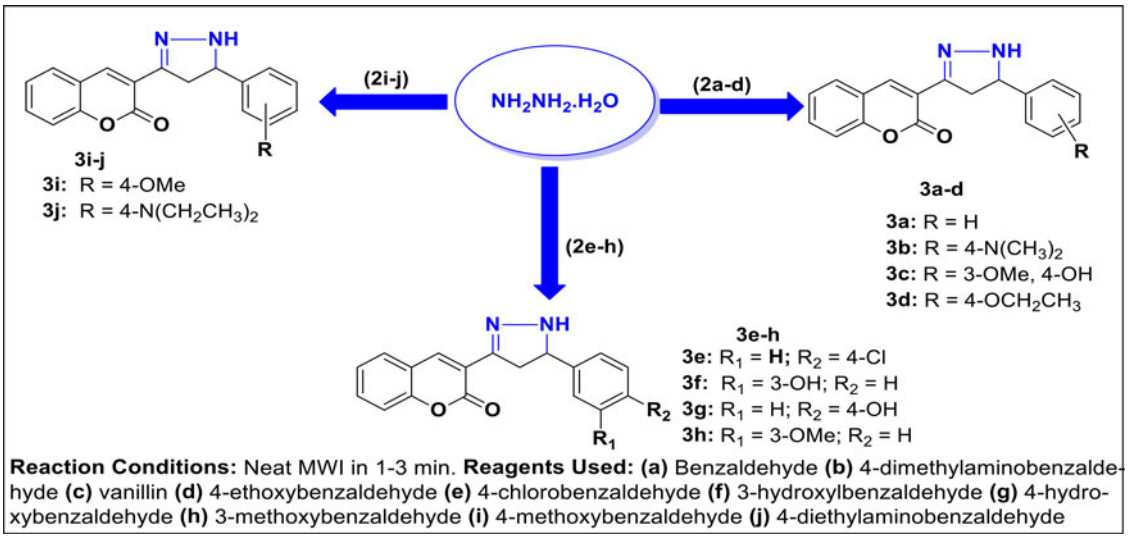

Scheme 3. Microwave-assisted synthesis of pyrazoline-linked coumarin, **3a-j.**

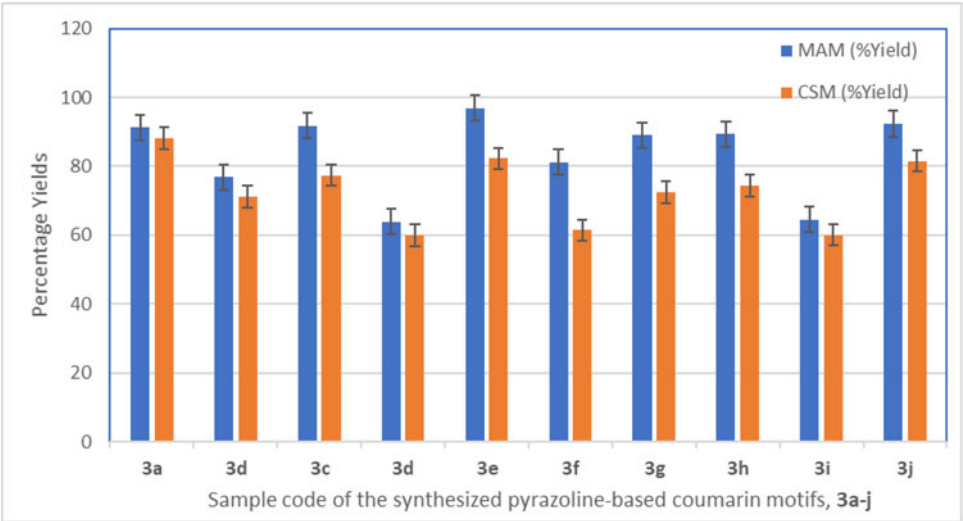

Figure 1. Comparative study of MAM and CSM using %yield descriptive indicator.

Table 1. Physico-chemical properties of precursor **1** and synthesized compounds **3a–j**.

Comp No	Molecular Formula	Mol. Weight	%Yield	Melting Point(°C)	Colour	Elemental analysis %Calcd. (%Found)		
						C	H	N
1	$C_{11}H_8O_3$	188.18	99.50	122–124	Yellow	70.10(69.97)	4.30(4.15)	–
3a	$C_{18}H_{14}N_2O_2$	290.32	91.28	111(s)	Orange	74.47(74.52)	4.86(5.00)	9.65(9.78)
3b	$C_{20}H_{19}N_3O_2$	333.38	76.82	152–154	Orange	72.05(71.89)	5.74(5.99)	12.60(12.83)
3c	$C_{19}H_{16}N_2O_4$	336.34	91.78	143–145	Orange	67.85(68.01)	4.79(4.94)	8.33(8.20)
3d	$C_{20}H_{18}N_2O_3$	334.37	63.93	120–121	Yellow	71.84(72.00)	5.43(5.62)	8.38(8.55)
3e	$C_{18}H_{13}N_2O_2Cl$	324.76	96.96	150–153	Yellow	66.57(66.75)	4.03(3.97)	8.63(8.70)
3f	$C_{18}H_{14}N_2O_3$	306.32	81.16	129–131	Brown	70.58(70.75)	4.61(4.80)	9.15(8.97)
3g	$C_{18}H_{14}N_2O_3$	306.32	89.03	140–141	Orange	70.58(70.70)	4.61(4.79)	9.15(8.91)
3h	$C_{19}H_{16}N_2O_3$	320.34	89.39	120–121	Orange	71.24(71.08)	5.03(4.94)	8.74(8.93)
3i	$C_{19}H_{16}N_2O_3$	320.34	64.60	117–119	Orange	71.24(71.12)	5.03(4.90)	8.74(8.55)
3j	$C_{22}H_{23}N_2O_3$	361.44	92.31	144–147	Orange	73.11(72.98)	6.41(6.60)	11.63(11.79)

Comp No = Compound number; Mol. Weight = Molecular weight; Calcd. = Calculated.

approach but also efficient, atom economical and highly productive for the synthesis of pyrazoline-linked coumarin **3a-j**.

The melting points ranged between 111 °C for compound **3a** to 152–154 °C for compound **3b.** Out of all the pyrazoline-based coumarin final products, **3a,** which was without any substituent on phenyl, had the lowest melting point. Hence, presence of substituent(s) on the phenyl ring might have contributed to increase in the melting points experience in compounds **3 b–j** as compared to **3a**. The virtual screening unveiled that the color varied from orange for **3a–c** and **3 g–j**; to yellow for **1, 3d** and **3e** with compound **3f** being the only brown colored compound (Table 1). The disparity in color with respect to **3f** might be because it was the only final product that possessed electron withdrawing group (EWG) as substituent on the phenyl ring. The progress of the reaction and the purity of the products were monitored through Thin Layer Chromatography (TLC) spotting using different solvent systems such as dichloromethane for the intermediates chalcones **2a–j** and Hexane: Ethyl acetate (9:1, v/v) as eluent for the final products **3a–j**. The elemental analytical data results for % calculated and % found for Carbon, Hydrogen and Nitrogen showed good agreement with constant difference of within ±0.25 (Table 1). The values were noticed to correlate well with molecular formula and weight parameters of the synthesized compounds **3a–j**.

3.1.2. Spectroscopic characterization

The structures of newly synthesized compounds were elucidated by UV, IR, ^{1}H- and ^{13}C-NMR as well as DEPT 135 spectroscopic data. The ^{1}H-NMR spectra of products **3a-j** was run at 400 MHz using DMSO-d_6. The most downfield signal was one proton singlet of phenolic OH at δ_H of 8.88–8.80 ppm, which was followed by the one proton singlet of heterocyclic part (coumarin) at δ_H of 8.69–8.61 ppm. All the aromatic protons resonated between δ_H of 7.96 ppm to 7.09 ppm which was in agreement with earlier reported value by Chavan & Hosamani, (2018). The NH proton resonated as doublet with δ_H values ranging from 6.94–6.91 ppm to 6.83–6.81 ppm. This confirms that the thermal cyclization resulted in pyrazoline (NH–CH) and not pyrazole. All other shielded protons were those of the aliphatic group and they appeared upfield between 3.40–3.36 ppm to 2.20 ppm. The result of ^{13}C-NMR was consistent with the total number of carbon atoms in compound **3a–j**. For instance, the ^{13}C-NMR spectrum of compound **3a** showed the presence of eighteen carbon atoms ranging from δ_C 195 ppm for C = O to δ_C 45.6 ppm for CH_2. Further confirmation of carbon type was ascertained via DEPT 135 NMR spectral data. It showed eleven positive signals from δ_C 147.0 ppm to δ_C 58.4 ppm which depicted numbers of methine (CH) carbon atoms in **3a**. The only negative signal in **3a** was at δ_C 45.6 ppm which showed that there was only one methylene carbon (CH_2) in the structure of pyrazoline-based coumarin **3a**. The electronic transition of uv-visible spectra in CH_2Cl_2 and DMSO for the intermediates chalcones **2a–j** and pyrazoline-based coumarin **3a–j** respectively gave rise to wavelength (λ_{max}) ranging from 205 nm to 461 nm (See experimental). The first set of wavelengths (λ_{max}) in each of the synthesized compounds were found between 207 and 220 nm and they were as a result of $\pi \rightarrow \pi^*$ transition of the compounds indicating the presence of C = C peculiar to benzene nucleus. This indicated that all the compounds possess benzene nucleus which was the benzenoid of coumarin. Each of all samples showed a peak at $\lambda_{max} > 200$ nm and < 300 nm. The uv-visible absorption spectrum of the precursor **1** showed a peak at $\lambda_{max} = 227$ nm (log $\varepsilon_{max} = 3.91$) and other two bathochromic shifts at $\lambda_{max} = 290$ nm and 335 nm (a shoulder) with log ε_{max} of 4.02 and 3.83 respectively. All the wavelength λ_{max} above benzenoid region (i.e. between 290 nm to 335 nm) was as a result of $\pi \rightarrow n$ transition due to contribution from C = O or C = N and extended conjugation by C = C groups. In addition, the highest wavelength 575 nm was found in the compound **3j**, which has 4-diethylamino group. This showed that the delocalization of the lone pair

of electrons on nitrogen into the benzene nucleus played a very contributing role to the bathochromic shift experienced by the compound **3j**. The infrared (IR) spectra of all the compounds were run in Bruker FT-IR. The infrared spectra of all the compounds **3a-j** showed absorption bands due to the stretching vibration of N-H of secondary amine, C-H aliphatic, C = O of ester, C = C of alkene, C = N at 3443–3412 cm^{-1}, 2980–2910 cm^{-1}, 1755–1745 cm^{-1}, 1620–1601 cm^{-1}, 1593–1572 cm^{-1} respectively. Other bending vibrational frequencies which served as confirmatory bands to some specific stretching bands were found at 1374–1362 cm^{-1} and 1228–1220 cm^{-1} depicting the presence of C-O and C-N functionalities respectively. The presence of specific broad bands at 3350–3345 cm^{-1} in compounds **3c, 3f** and **3 g** was due to presence of OH of phenol in those compounds. The prove of a successful conversion of carbonyl of acetyl **1** to pyrazoline-based coumarins **3a–j** could be established by the presence of the C = O of conjugated ketone (C = C-$COCH_3$) at 1685 cm^{-1} in starting material **1** which disappeared in the bands of all the products **3a–j**.

3.2 Antibacterial activities

3.2.1. General in vitro sensitivity testing

Antibacterial assay was prepared according to standard method described in experimental section (Ajani et al., 2010; Ajani & Nwinyi, 2010). Gentamicin was used as reference drug for the antibacterial activities according to standard method (Ajani et al., 2010; Ajani & Nwinyi, 2010). The mode of action of gentamicin entailed irreversible binding at ribosomal level, thereby signaling to interrupt and truncate protein synthesis which was the rationale for choosing gentamicin as the clinical standard (Prescott et al., 2005). The result of antibacterial screening (Sensitivity testing) on bacteria with zones of inhibition in mm is as presented in Table 2. The used precursor **1**, targeted products **3a–j** and gentamicin standard were screened *in vitro* against six bacterial isolates which were two gram positive {*Staphylococcus aureus* (ATCC 25923) and *Streptococcus faecalis* (LIO)}, and four gram negative {*Klebsiella pneumonia* (ATCC 13182), *Proteus vulgaris* (LIO), *Pseudomonas aeruginosa* (ATCC 15442), *Escherichia coli* (25922)} using agar diffusion method. The zones of inhibition recorded for precursor **1** against the six organisms was from 6.00 ± 0.55 mm for *E. coli* to 12.00 ± 0.69 mm for *K. pneumonia* while that of titled compounds **3a-j** was from 8.00 ± 0.64 mm for **3a** in *E. coli* to 32.00 ± 1.01 mm for **3h** in *S. aureus*. Gentamicin standard showed activity against all the bacteria with the zones of inhibition ranging from 4.00 ± 0.33 mm for *E. coli* to 18.00 ± 0.88 mm for *P. vulgaris*. From the growth inhibition trend based on the measured Z.O.I. pattern, pyrazoline-based coumarins **3a–j** had larger Z.O.I. than precursor **1** which was in turn had larger Z.O.I. than gentamicin. This revealed that synthetic transformation of precursor **1** via functional groups interconversion to the envisaged coumarin motifs **3a–j** was a rich-rewarding exercise because compound **1** was never a match for the **3a–j** in their sensitivity potentials. This suggested that the synthesized compounds **3a–j** could probably be a viable replacement or bioactive enhancer for gentamicin in efficient drug design. There were large zones of inhibition which culminated into broad spectrum of activity as shown in the plates depicting activities of some selected compounds against some selected bacterial strains (Figure 2).

Furthermore, the result of activity index (A.I.) of the precursor **1** and the pyrazoline-based coumarin motifs **3a–j** as compared with gentamicin standard is as shown in Table 3. All the final products **3a–j** had higher activity indices (1.60–3.20) than gentamicin whereas precursor **1** had similar A.I. with the standard against *S. aureus*. Measuring the activity index against *S. faecalis* revealed that only **1** had a lower activity index (0.67) than the standard while **3e** was equal in A.I. with the standard and all other targeted products **3a–d** and **3f–j** were higher in their activity indices (1.33–2.00) than the standard (1.00). It is interesting to note that all compounds possessed better activity indices than the gentamicin drug against *K. pneumonia* (1.71–3.86) and *E. coli* (1.50–7.50) which were both gram-negative organisms. Members of the *Klebsiella* genus and *E. coli* typically express two types of antigens on their cell surfaces. The first, O-antigen, is a component of the lipopolysaccharide (LPS) which plays crucial role in antimicrobial susceptibility of *E. coli* and possessed nine varieties (Ebbensgaard et al., 2018). The second is K antigen, a capsular polysaccharide with more than 80 varieties. Both contribute to pathogenicity and form the basis for serogroup (DebRoy et al., 2016). The effect of the presence of pyrazoline on the coumarin scaffolds was also investigated by the comparative study of the activity of the non-pyrazolinized coumarin (chalcone) **2a** to that of the pyrazoline-linked coumarin counterpart **3a** as shown the Figure 3. The zones of inhibition of **3a** on all the organisms was appreciably higher than that of **2a** except in *Klebsiella pneumonia* alone which might be as a result of the mechanism of action of this gram-negative organism and available K antigen with a capsular polysaccharide nature in it (DebRoy et al., 2016). It was also interesting to note that both *Staphylococcus aureus* and *Pseudomonas aeruginosa* developed resistance against action of non-

Table 2. Antibacterial screening (sensitivity testing) on bacteria with zones of inhibition (mm).

Bacteria → Comp. No↓	*S. aureus*	*S. faecalis*	*K. pneumonia*	*P. vulgaris*	*P. aeruginosa*	*E. coli*
1	10.00 ± 0.63	10.00 ± 0.61	12.00 ± 0.69	07.00 ± 0.60	07.00 ± 0.58	06.00 ± 0.55
3a	16.00 ± 0.83	22.00 ± 0.93	14 .00 ± 0.74	19.00 ± 0.88	12.00 ± 0.73	8.00 ± 0.64
3b	16.00 ± 0.82	20.00 ± 0.88	12.00 ± 0.71	10.00 ± 0.63	8.00 ± 0.60	12.00 ± 0.71
3c	16.00 ± 0.84	20.00 ± 0.89	16.00 ± 0.83	19.00 ± 0.89	14.00 ± 0.73	18.00 ± 0.87
3d	24.00 ± 0.92	28.00 ± 0.98	22.00 ± 0.91	22.00 ± 0.92	17.00 ± 0.87	22.00 ± 0.89
3e	16.00 ± 0.84	15.00 ± 0.83	14.00 ± 0.79	20.00 ± 0.89	12.00 ± 0.72	12.00 ± 0.72
3f	32.00 ± 1.00	26.00 ± 0.97	22.00 ± 0.90	26.00 ± 0.96	22.00 ± 0.92	24.00 ± 0.93
3g	28.00 ± 0.98	30.00 ± 0.99	27.00 ± 0.97	28.00 ± 0.98	29.00 ± 0.98	28.00 ± 0.98
3h	32.00 ± 1.01	20.00 ± 0.88	26.00 ± 0.98	28.00 ± 0.99	18.00 ± 0.88	30.00 ± 0.99
3i	22.00 ± 0.92	28.00 ± 0.99	20.00 ± 0.88	22.00 ± 0.92	22.00 ± 0.91	20.00 ± 0.89
3j	16.00 ± 0.85	22.00 ± 0.92	20.00 ± 0.89	20.00 ± 0.88	16.00 ± 0.85	08.00 ± 0.62
Gtm	10.00 ± 0.64	15.00 ± 0.83	07.00 ± 0.59	18.00 ± 0.88	12.00 ± 0.73	04.00 ± 0.33

Mean ± SD of triplicate measurements, S. aureus = Staphylococcus aureus (ATCC 25923: G^+), S. faecalis = Streptococcus faecalis (LIO: G^+), K. pneumonia = Klebsiella pneumonia (ATCC 13182: G^-), P. vulgaris = Proteus vulgaris (LIO: G^-), P. aeruginosa = Pseudomonas aeruginosa (ATCC 15442: G^-), E. coli = Escherichia coli (ATCC 25922: G^-), G^+ = Gram-positive, G^- = Gram-negative, Gtm = Gentamicin; ATCC = American Type Culture Collection, LIO = Locally Isolated Organism.

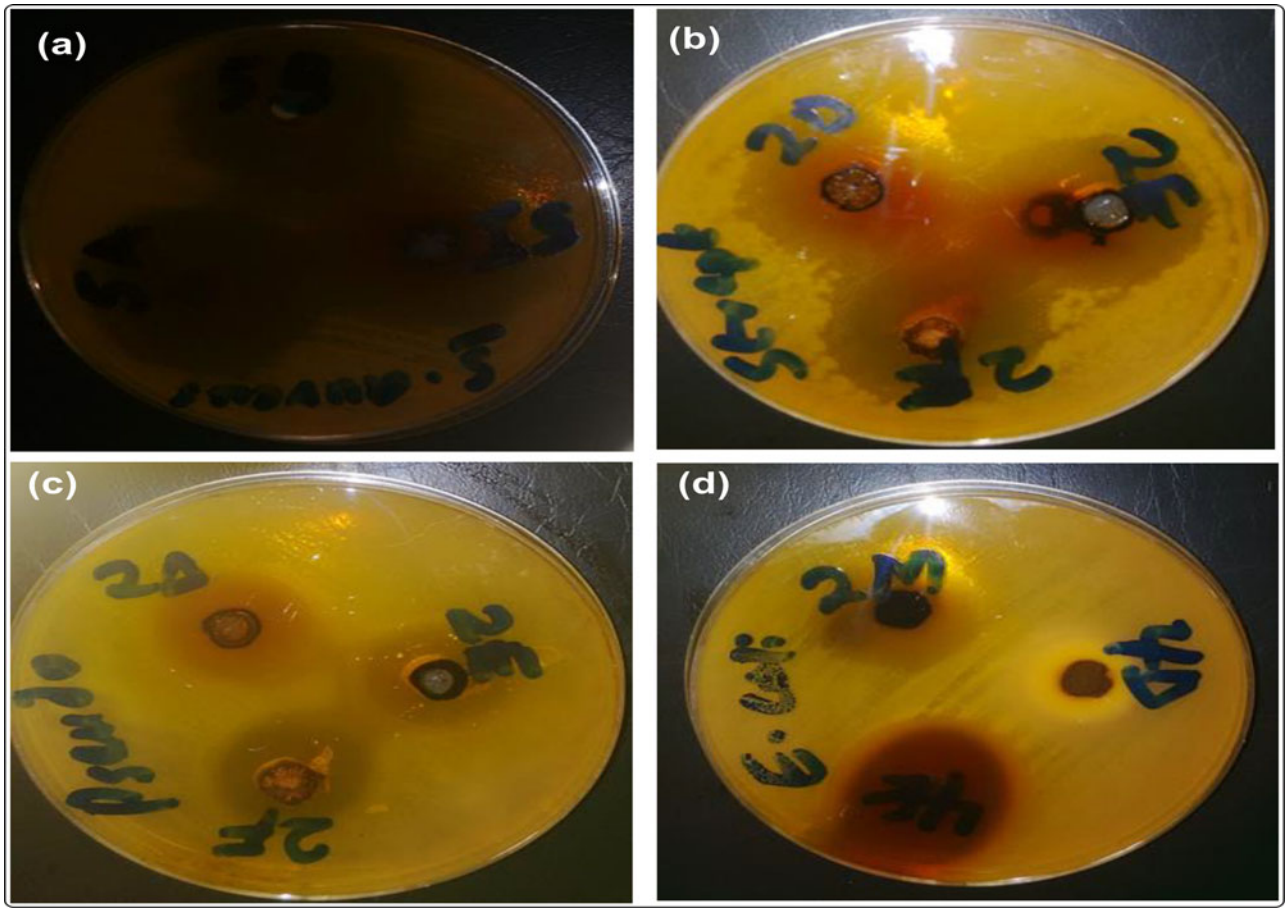

Figure 2. The plates showing the zones of inhibition of susceptibility of: (a) *S. aureus* against **5a, 5 b** and **5i** with new codes of **3a, 3 b,** and **3c** respectively (b) *S. faecalis* against **2d, 2e** and **2f** with new codes of **3d, 3 g,** and **3j** respectively (c) *P. aeruginosa* against **2d, 2e** and **2f** with new codes of **3d, 3 g,** and **3j** respectively (d) *E.coli* against **2 m, 4d** and **4e** with new codes of **3f, 3e,** and **3 h** respectively.

pyrazolinized-coumarin (chalcone) **2a** whereas pyrazoline-bearing coumarin **3a** strongly inhibited the growth of these two organisms with notable large zones of inhibition of 16 mm and 12 mm respectively (Figure 3). It was earlier reported by Zhang et al. (2014) that imidazoles-linked coumarin proved to be more promising compounds than fadrozole standard drug as CYP450 inhibitors. The result herein obtained with pyrazoline-linked coumarin agreed with the findings of Zhang et al. (2014), because the pyrazoline-linked coumarin **3a** exhibited a higher antibacterial activity than the non-pyrazolinized coumarin (chalcone **2a**). Hence, the use of pyrazoline as a linker between the coumarin heterocycle and substituted phenyl groups was a worthwhile adventure for bioactivity enhancement of these biomolecules.

3.2.2. MIC and MBC activities testing

In addition, minimum inhibitory concentration (MIC) test of pyrazoline-based coumarins **3a–j** was carried out on six organisms using Ajani, Iyaye, et al. (2018) method as shown in Table 4. The result excluded

Table 3. The activity index of the synthesized compounds against the targeted organisms.

Bacteria → Comp. No↓	*S. aureus*	*S. faecalis*	*K. pneumonia*	*P. vulgaris*	*P. aeruginosa*	*E. coli*
1	1.00 ± 0.03	0.67 ± 0.02	1.71 ± 0.05	0.39 ± 0.02	0.58 ± 0.02	1.50 ± 0.06
3a	1.60 ± 0.05	1.47 ± 0.05	2.00 ± 0.05	1.06 ± 0.05	1.00 ± 0.05	2.00 ± 0.05
3b	1.60 ± 0.06	1.33 ± 0.05	1.71 ± 0.05	0.56 ± 0.02	0.67 ± 0.02	3.00 ± 0.10
3c	1.60 ± 0.05	1.33 ± 0.03	2.29 ± 0.07	1.06 ± 0.03	1.17 ± 0.04	4.50 ± 0.10
3d	2.40 ± 0.09	1.87 ± 0.07	3.14 ± 0.10	1.22 ± 0.04	1.42 ± 0.06	5.50 ± 0.12
3e	1.60 ± 0.05	1.00 ± 0.03	2.00 ± 0.06	1.11 ± 0.04	1.00 ± 0.04	3.00 ± 0.09
3f	3.20 ± 0.09	1.73 ± 0.05	3.14 ± 0.09	1.44 ± 0.03	1.83 ± 0.06	6.00 ± 0.14
3g	2.80 ± 0.08	2.00 ± 0.06	3.86 ± 0.10	1.56 ± 0.04	2.42 ± 0.07	7.00 ± 0.14
3h	3.20 ± 0.10	1.33 ± 0.04	3.71 ± 0.10	1.56 ± 0.05	1.50 ± 0.05	7.50 ± 0.15
3i	2.20 ± 0.07	1.87 ± 0.06	2.86 ± 0.09	1.22 ± 0.04	1.83 ± 0.06	5.00 ± 0.13
3j	1.60 ± 0.05	1.47 ± 0.04	2.86 ± 0.08	1.11 ± 0.05	1.33 ± 0.05	2.00 ± 0.07
Gtm	1.00 ± 0.04	1.00 ± 0.04	1.00 ± 0.04	1.00 ± 0.04	1.00 ± 0.04	1.00 ± 0.04

Comp. No = compound number; Mean ± SD of triplicate measurements, *S. aureus* = *Staphylococcus aureus* (ATCC 25923: G^+), *S. faecalis* = *Streptococcus faecalis* (LIO: G^+), *K. pneumonia* = *Klebsiella pneumonia* (ATCC 13182: G^-), *P. vulgaris* = *Proteus vulgaris* (LIO: G^-), *P. aeruginosa* = *Pseudomonas aeruginosa* (ATCC 15442: G^-), *E. coli* = *Escherichia coli* (ATCC 25922: G^-), G^+ = Gram-positive, G^- = Gram-negative, Gtm = Gentamicin; ATCC = American Type Culture Collection, LIO = Locally Isolated Organism.

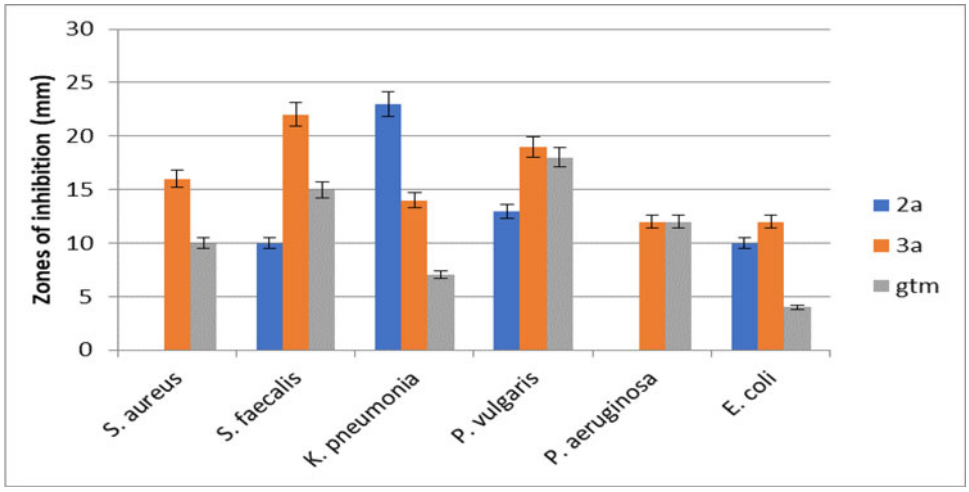

Figure 3. Comparative study of activity of chalcone **2a** and pyrazoline-coumarin counterpart **3a**.

Table 4. Results of minimum inhibitory concentration (MIC) of **3a-j** on bacteria (μg/mL).

Bacteria → Comp. No↓	*S. aureus*	*S. faecalis*	*K. pneumonia*	*P. vulgaris*	*P. aeruginosa*	*E. coli*
3a	31.25 ± 1.08	62.50 ± 2.00	31.25 ± 0.85	31.25 ± 0.85	125.00 ± 3.00	62.50 ± 2.02
3b	31.25 ± 1.07	62.50 ± 2.00	125.00 ± 3.03	62.50 ± 2.02	250.00 ± 3.90	250.00 ± 3.90
3c	125.00 ± 2.98	62.50 ± 2.00	62.50 ± 2.02	62.50 ± 2.02	125.00 ± 3.01	250.00 ± 3.92
3d	15.63 ± 0.92	62.50 ± 2.00	62.50 ± 2.02	31.25 ± 0.87	250.00 ± 3.90	62.50 ± 2.00
3e	31.25 ± 0.84	125.00 ± 3.02	62.50 ± 2.00	62.50 ± 2.02	250.00 ± 3.92	31.25 ± 0.87
3f	62.50 ± 2.00	62.50 ± 2.00	125.00 ± 3.03	62.50 ± 2.02	250.00 ± 3.90	62.50 ± 2.00
3g	62.50 ± 2.08	7.82 ± 0.43	125.00 ± 3.01	15.63 ± 0.92	7.82 ± 0.42	62.50 ± 2.00
3h	3.91 ± 0.22	62.50 ± 2.00	125.00 ± 3.01	125.00 ± 3.01	125.00 ± 3.00	125.00 ± 3.01
3i	125.00 ± 3.01	62.50 ± 2.00	125.00 ± 3.00	62.50 ± 2.00	250.00 ± 3.90	62.50 ± 2.00
3j	3.91 ± 0.22	3.91 ± 0.22	15.63 ± 0.94	15.63 ± 0.92	31.25 ± 0.87	7.82 ± 0.43

S. aureus = *Staphylococcus aureus* (ATCC 23235: G^+), *S. faecalis* = *Streptococcus faecalis* (ATCC 29212: G^+), *K. pneumonia* = *Klebsiella pneumonia* (ATCC 13882: G^-), *P. vulgaris* = *Proteus vulgaris* (ATCC 29905: G^-), *P. aeruginosa* = *Pseudomonas aeruginosa* (ATCC 10145: G^-), *E. coli* = *Escherichia coli* (ATCC 8739: G^-), G^+ = Gram positive, G^- = Gram negative, Gtm = Gentamicin.

that of precursor **1** because of its low zones of inhibition recorded in general sensitivity testing (Table 2) and activity index results (Table 3). The MIC values of growth inhibitory potential of **3a–j** against gram-positive organisms *S. aureus* and *S. faecalis* varied from 3.91 ± 0.22 μg/mL to 125.00 ± 3.02 μg/mL; for gram-negative organisms *K. pneumonia* and *P. vulgaris*, it ranged from 15.63 ± 0.94 μg/mL to 125.00 ± 3.01 μg/mL; and for the last two gram-negative bacterial isolates *P. aeruginosa* and *E. coli*, the MIC ranges were recorded to be 7.82 ± 0.43 μg/mL to 250.00 ± 3.92 μg/mL. The efficiency of **3a–j** was lowest against growth inhibition of *P. aeruginosa* with very high MIC values of 125 μg/mL to 250 μg/mL except for **3 g** (MIC = 7.82 μg/mL) and **3j** (MIC = 31.25 μg/mL). This may be explained by the hardy cell wall of this organism which contains porins and efflux pumps called ABC transporters, known to be notoriously responsible for pumping out of some antibiotics before they are able to act. It may also be due to the protective biofilms formed by these organisms (Prescott et al., 2005). Upon comparing the efficacious trend of series of compounds **3a–j** across board the bacterial isolates screened, **3j**

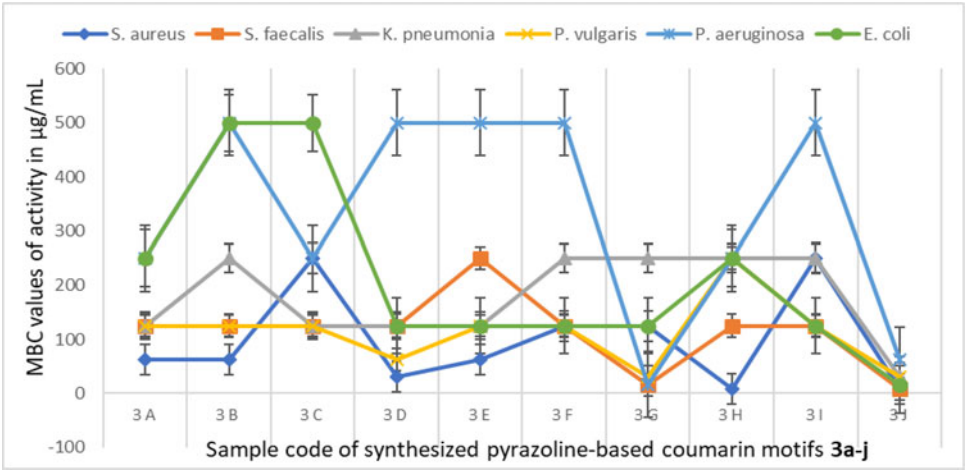

Figure 4. Graphical representation of minimum bactericidal concentration (MBC) of **3a–j**.

(MIC = 3.91 ± 0.22 µg/mL) was noticed to be more active than **3a–i** (MIC > 3.91 µg/mL) against *S. aureus* and *S. faecalis*; **3j** (MIC = 7.82 ± 0.43 µg/mL) was more effective than **3a–i** (MIC > 7.82 µg/mL) against *E. coli*; **3j** (MIC = 15.63 ± 0.94 µg/mL) was more active than **3a–i** (MIC > 15.63 µg/mL) against *K. pneumonia* and *P. vulgaris*; **3j** (MIC = 31.25 ± 0.87 µg/mL) was more potent than **3a–i** (MIC > 31.25 µg/mL) against *P. aeruginosa*. The pyrazoline-based coumarin **3j** was the most active with the lowest MIC against all the four gram-negative and two gram-positive organisms used herein. The minimum bactericidal concentration (MBC) testing was determined on the series of pyrazoline-linked coumarin motifs **3a–j** against tested organisms to authenticate the lowest concentration of the coumarin solution that causes death of the organisms under the investigation (Figure 4). The MBC ranged from 7.82 µg/mL to 500 µg/mL. All MBC values were observed to be two folds higher than the MIC expect in the case of non-substituted phenyl **3a** against *K. pneumonia* and *P. vulgaris* and electron withdrawing group (Cl) substituted phenyl **3e** against *E. coli* where MBC values were four folds higher than the MIC.

3.2.3. Structure activity relationship (SAR) study

In order to optimize the inhibitory potential of targeted coumarin motifs **3a–j** and to comprehend which substituent(s) on phenyl is/are essential for the bioactivity, ten structurally related analogs were synthetically achieved by thermal cyclization of chalcone **2a–j** via hydrazinolysis pathway to access pyrazoline-linked coumarin motifs **3a–j.** The potency of the inhibitions against *S. aureus* decreased in the following order: **3j ≈ 3 h » 3d > 3a ≈ 3 b ≈ 3e > 3f ≈ 3 g > 3c ≈ 3i.** This depicted that π-π stacking character in 2*H*-chromen-2-one core skeleton of coumarin worked synergistically with electron donating ability of electron donating groups (EDGs) to cause activity boosting against growth potential of *S. aureus*. Based on the *in vitro* screening of **3a–j** against *S. faecalis*, the order of activity was **3j > 3 g » 3a-d ≈ 3f ≈ 3 h ≈ 3i > 3e.** This is a strong indication that presence of EWG (Cl) at 4-position as seen in **3e** led to experiencing poor activity against *S. faecalis*. The order of tolerability and susceptibility of *K. pneumonia* to coumarin **3a**-j showed that **3j > 3a > 3c–e ≈ 3 b ≈ 3f–i.** The order of activity against *P. aeruginosa* was **3 g > 3j » 3a ≈ 3c ≈ 3 h > 3 b ≈ 3d-f ≈ 3i** while the trend of activity variation against the last gram-negative organism, *E. coli* was **3j » 3e > 3a ≈ 3d ≈ 3f ≈ 3 g ≈ 3i > 3 h > 3 b ≈ 3c.** This SAR study showed that a substitution is well tolerated in 3- and 4-positions template containing electron donating groups (EDG: NR_2, OH, OEt, OMe), whereas it is less tolerated when the substituent was electron withdrawing (EWG: Cl). The Table 4 together with Figure 4 highlighted these findings by synopsizing all changes and their outcomes in activity retention or loss. Addition of a methoxy group in 3- and 4-positions as in **3c**. **3h, 3i** was well tolerated, as well as exchanging this moiety to hydroxyl as in **3c, 3f, 3g**. Apparently, only EDG was accepted at position-4, because changing the features at this position to chlorine (EWG in **3e**) led to weakening or reduction of potency in **3e** as compared to other analogs in this series. Analog **3j** showed highest potency against all six organisms and emerged as the most active antibacterial agent with MIC of 3.92 µg/mL, surpassing the potency of the gentamicin which was used clinical standard and positive control in all measurements.

4. Conclusion

Toxicity of the reacting solvents and the discharge of poisonous chemicals associated with conventional synthesis of coumarin derivative was herein overcome by using microwave irradiation in solvent-free medium as eco-friendly and as greener approach towards accessing the targeted pyrazoline-based coumarin derivatives **3a–j**. Pyrazoline-linked coumarin derivatives, **3a–j** were successfully synthesized

within very short reaction time and in good to excellent yields. Finally, the synthesized compounds **3a–j** exhibited strong inhibitory efficiencies, most of which were even higher than that of the gentamicin which was the standard antibiotic used as the positive control. Compound **3j** emerged as the most potent antibacterial agent having MIC and MBC values of $3.92 \pm 0.22\,\mu g/mL$ and $7.82 \pm 0.43\,\mu g/mL$ respectively. These analogs exhibit good candidature for further study to ascertain the toxicological profile which might open new window of opportunity to novel drug design.

Acknowledgements

The World Academy of Sciences (TWAS) is gratefully acknowledged for the sponsorship of this project under the TWAS Research Grant for individual Programme (Grant No. 14-069 RG/CHE/AF/AC_1).

Disclosure statement

The authors declare that there is no conflict of interest regarding this publication.

ORCID

Tolutope O. Siyanbola http://orcid.org/0000-0002-8406-6167
Damilola V. Aderohunmu http://orcid.org/0000-0002-3563-2919
Anuoluwa A. Akinsiku http://orcid.org/0000-0001-8657-0837
Shade J. Olorunshola http://orcid.org/0000-0002-0185-0213

References

Acar, M., Bozkurt, E., Meral, K., Arik, M., & Onganer, Y. (2015). The fluorescence quenching mechanism of coumarin 120 with CdS nanoparticles in aqueous suspension. *Journal of Luminescence*, *157*, 10–15.

Ajani, O. O. (2014). Present status of quinoxaline motifs: Excellent pathfinders in therapeutic medicine. *European Journal of Medicinal Chemistry*, *85*, 688–715.

Ajani, O. O., Ajayi, O., Adekoya, J. A., Owoeye, T. F., Durodola, B. M., & Ogunleye, O. M. (2016). Comparative study of microwave-assisted and conventional synthesis of 3-[1-(s-phenylimino) ethyl]-2*H*-chromen-2-ones and selected hydrazone derivatives. *Journal of Applied Sciences*, *16*(3), 77–87.

Ajani, O. O., Aderohunmu, D. V., Owolabi, F. E., Olomieja, A. O., & Jolayemi, E. G. (2018). Microwave assisted synthesis of pyrazoline-based coumarin derivatives: A comparative study. *J. Chem. Soc. Nigeria*, *43*(1), 134–139.

Ajani, O. O., Iyaye, K. T., Audu, O. Y., Olorunshola, S. J., Kuye, A. O., & Olanrewaju, I. O. (2018). Microwave assisted synthesis and antimicrobial potential of quinoline-based 4-hydrazide-hydrazone derivatives. *Journal of Heterocyclic Chemistry*, *55*(1), 302–312.

Ajani, O. O., & Nwinyi, O. C. (2010). Microwave assisted synthesis and evaluation of antimicrobial activity of 3-{3-(s-aryl and s-heteroaromatic) acryloyl}-2*H*-chrom en-2-one derivatives. *Journal of Heterocyclic Chemistry*, *47*, 179–187.

Ajani, O. O., Obafemi, C. A., Nwinyi, O. C., & Akinpelu, D. A. (2010). Microwave assisted synthesis and antimicrobial activity of 2-quinoxalinone-3-hydrazone derivatives. *Bioorganic & Medicinal Chemistry*, *18*(1), 214–221.

Amin, K. M., Taha, A. M., George, R. F., Mohamed, N. M., & Elsenduny, F. F. (2018). Synthesis, antitumor activity evaluation, and DNA-binding study of coumarin-based agents. *Archiv Der Pharmazie*, *351*, 1700199. doi:10.1002/ardp.201700199.

Aslam, B., Wang, W., Arshad, M. I., Khurshid, M., Muzammil, S., Rasool, M. H., … Baloch, Z. (2018). Antibiotic resistance: A rundown of a global crisis. *Infection and Drug Resistance*, *11*, 1645–1658.

Bansal, Y., Sethi, P., & Bansal, G. (2013). Coumarin: A potential nucleus for anti-inflammatory molecules. *Medicinal Chemistry Research*, *22*(7), 3049–3060.

Bouhenna, M. M., Perez, M. V., Talhi, O., Bachari, K., Silva, A. M. S., Luyten, W., & Mameri, N. (2018). Anticancer activity study of chromone and coumarin hybrids using electrical impedance spectroscopy. *Anti-Cancer Agents in Medicinal Chemistry*, *18*(6), 854–864. doi:10.2174/1871520618666180130102259.

Chatterjee, A., & Seth, D. (2013). Photophysical properties of 7-(diethylamino)coumarin-3-carboxylic acid in the nanocage of cyclodextrins and in different solvents and solvent mixtures. *Photochemistry and Photobiology*, *89*(2), 280–293.

Chavan, R. R., & Hosamani, K. M. (2018). Microwave-assisted synthesis, computational studies and antibacterial/ anti-inflammatory activities of compounds based on coumarin-pyrazole hybrid. *Royal Society Open Science*, *5*(5), 172435. doi:10.1098/rsos.172435.

Cui, Y. J., Tang, L. Q., Zhang, C. M., & Liu, Z. P. (2019). Synthesis of novel pyrazole derivatives and their tumor cell growth inhibitory activity. *Molecules*, *24*(2), 279. doi:10.3390/molecules24020279.

DebRoy, C., Fratamico, P. M., Yan, X., Baranzoni, G., Liu, Y., Needleman, D. S., … Katani, R. (2016). Comparison of O-antigen gene clusters of all O-serogroups of *Escherichia coli* and proposal for adoptiga new nomenclature for O-typing. *PLoS One*, *11*(4), e0154551.

de la Hoz, A., Diaz-Ortiz, A., & Prieto, P. (2016). Microwave-assisted green organic synthesis. Chapter 1. In G. Stefanidis & A. Stankiewicz (Eds.), *Alternative Energy Sources for Green Chemistry* (pp. 1–34). Cambridge, UK: Royal Society of Chemistry.

Delcourt, M. L., Reynaud, C., Turcaud, S., Favereau, L., Crassous, J., Micouin, L., & Benedetti, E. (2019). 3D Coumarin systems based on [2.2]paracyclophane: Synthesis, spectroscopic characterization, and chiroptical properties. *The Journal of Organic Chemistry*, *84*(2), 888–899.

El Azab, I. H., Ali, O. A. A., El-Zahrani, A. H., Gobouri, A. A., & Altalhi, T. A. (2019). Pyrazole-1-carbothioamide as a potent precursor for synthesis of some new n-heterocycles of potential biological activity. *Journal of Heterocyclic Chemistry*, *56*(1), 18–21.

Ebbensgaard, A., Mordhorst, H., Aarestrup, F. M., & Hansen, E. B. (2018). The role of outer membrane protein and lipopolysaccharides for the sensitivity of *Escherichia coli* to antimicrobial peptides. *Front. Microbiol*, *9*, 2153. doi:10.3389/fmicb.2018.02153.

Gedye, R., Smith, F., Westaway, K., Ali, H., Baldisera, L., Laberge, L., & Rousell, J. (1986). The use of microwave ovens for rapid organic synthesis. *Tetrahedron Letters*, *27*(3), 279–282.

Gude, V. G., Patil, P., Martinez-Guerra, E., Deng, S., & Nirmalakhandan, N. (2013). Microwave energy potential for biodiesel production. *Sustainable Chemical Processes*, *1*, 5. doi:10.1186/2043-7129-1-5.

Gümüş, M. K., & Elemes, Y. (2018). Eco-friendly synthesis of novel thiohydantoin-type sulfur-containing imidazolinone derivatives from glycine ester. *Chemistry of Heterocyclic Compounds*, *54*(2), 153–157.

Hu, X. L., Gao, C., Xu, Z., Liu, M. L., Feng, L. S., & Zhang, G. D. (2018). Recent development of coumarin derivatives as potential antiplasmodial and antimalarial agents. *Current Topics in Medicinal Chemistry*, *18*(2), 114–123.

Iyer, D., & Patil, U. K. (2014). Evaluation of antihyperlipidemic and antitumor activities of isolated coumarins from *Salvadora indica*. *Pharmaceutical Biology*, *52*(1), 78–85.

Kale, M., & Patwardhan, K. (2014). Pharmacological significance of coumarin-linked heterocycles: A review. *Journal of Current Pharma Research*, *4*(2), 1150–1158.

Muhammad, N., Saeed, M., Khan, H., Adhikari, A., & Khan, K. M. (2013). Muscle relaxant and sedative-hypnotic activities of extract of *Viola betonicifolia* in animal models supported by its isolated compound, 4-hydroxy coumarin. *Journal of Chemistry*, *2013*, 326263. doi:10.1155/2013/326263.

Patel, R. V., Kumari, P., Rajani, D. P., & Chikhalia, K. H. (2013). Synthesis of coumarin-based 1,3,4-oxadiazol-2ylthio-*N*-phenyl/benzothiazolyl acetamides as antimicrobial and antituberculosis agents. *Medicinal Chemistry Research*, *22*(1), 195–210.

Patil, P. O., Bari, S. B., Firke, S. D., Deshmukh, P. K., Donda, S. T., & Patil, D. A. (2013). A comprehensive review on synthesis and designing aspects of coumarin derivatives as monoamine oxidase inhibitors for depression and Alzheimer's disease. *Bioorganic & Medicinal Chemistry*, *21*(9), 2434–2450.

Pawełczyk, A., Sowa-Kasprzak, K., Olender, D., & Zaprutko, L. (2018). Molecular consortia-various structural and synthetic concepts for more effective therapeutics synthesis. *International Journal of Molecular Sciences*, *19*(4), 1104. doi:10.3390/ijms19041104.

Peng, H. K., Chen, W. C., Lee, J. C., Yang, S. Y., Tzeng, C. C., Lin, Y. T., & Yang, S. C. (2013). Novel anilinocoumarin derivatives as agents against hepatitis C virus by the induction of IFN-mediated antiviral responses. *Organic & Biomolecular Chemistry*, *11*(11), 1858–1866.

Pereira, T. M., Franco, D. P., Vitorio, F., & Kummerle, A. E. (2018). Coumarin compounds in medicinal chemistry: Some important examples from the last years. *Current Topics in Medicinal Chemistry*, *18*(2), 124–148.

Pérez-Cruz, K., Moncada-Basualto, M., Morales-Valenzuela, J., Barriga-González, G., Navarrete-Encina, P., Núñez-Vergara, L., … Olea-Azar, C. (2018). Synthesis and antioxidant study of new polyphenolic hybrid-coumarins. *Arabian Journal of Chemistry*, *11*(4), 525–537.

Prescott, L. M., Harley, J. P., & Donald, K. A. (2005). *In microbiology*. 6th ed. New York: McGraw Hill.

Song, X. Y., Hu, J. F., Sun, M. N., Li, Z. P., Wu, D. H., Ji, H. J., … Chen, N. H. (2013). IMM-H004, a novel coumarin derivative compound, protects against amyloid beta-induced neurotoxicity through a mitochondrial-dependent pathway. *Neuroscience*, *242*, 28–38.

Srivastav, V. K., Tiwari, M., Zhang, X., & Yao, X. J. (2018). Synthesis and antiretroviral activity of 6-acetyl-coumarin derivatives against HIV-1 infection. *Indian Journal of Pharmaceutical Sciences*, *80*(1), 108–117.

Stefanachi, A., Leonetti, F., Pisani, L., Catto, M., & Carotti, A. (2018). Coumarin: A natural, privileged and versatile scaffold for bioactive compounds. *Molecules*, *23*, 250. doi:10.3390/molecules23020250.

Venkateswarlu, V., Kour, J., Kumar, K. A. A., Verma, P. K., Reddy, G. L., Hussain, Y., … Sawant, S. D. (2018). Direct *N*-heterocyclization of hydrazines to access styrylated pyrazoles: Synthesis of 1,3,5-trisubstituted pyrazoles and dihydropyrazoles. *RSC Advances*, *8*(47), 26523–26527.

Wei, Y., Miao, K. L., & Hao, S. H. (2018). Novel 4-methylumbelliferone amide derivatives: Synthesis, characterization and pesticidal activities. *Molecules*, *23*(1), 122. doi:10.3390/molecules23010122.

Widelski, J., Luca, S. V., Skiba, A., Chinou, I., Marcourt, L., Wolfender, J. L., & Skalicka-Wozniak, K. (2018). Isolation and antimicrobial activity of coumarin derivatives from fruits of *Peucedanum luxurians* tamamsch. *Molecules*, *23*(5), 1222. doi:10.3390/molecules23051222.

Yue, C., Fang, D., Liu, L., & Yi, T. F. (2011). Synthesis and application of task-specific ionic liquids used as catalysts and/or solvents in organic unit reactions. *Journal of Molecular Liquids*, *163*(3), 99–121.

Zhang, L., Peng, X. M., Damu, G. L., Geng, R. X., & Zhou, C. H. (2014). Comprehensive review in current developments of imidazole-based medicinal chemistry. *Medicinal Research Reviews*, *34*(2), 340–437.